Reports

Sea Surface Temperature, Surface Wind Divergence, and Convection over Tropical Oceans

N. E. GRAHAM AND T. P. BARNETT

Large-scale convection over the warm tropical oceans provides an important portion of the driving energy for the general circulation of the atmosphere. Analysis of regional associations between ocean temperature, surface wind divergence, and convection produced two important results. First, over broad regions of the Indian and Pacific oceans, sea surface temperatures (SSTs) in excess of 27.5°C are required for large-scale deep convection to occur. However, SSTs above that temperature are not a sufficient condition for convection and further increases in SST appear to have little effect on the intensity of convection. Second, when SSTs are above 27.5°C, surface wind divergence is closely associated with the presence or absence of deep convection. Although this result could have been expected, it was also found that areas of persistent divergent surface flow coincide with regions where convection appears to be consistently suppressed even when SSTs are above 27.5°C. Thus changes in atmospheric stability caused by remotely forced changes in subsidence aloft may play a major role in regulating convection over warm tropical oceans.

WE HAVE STUDIED OBSERVATIONS of sea surface temperature (SST), atmospheric convection, and surface wind divergence from the tropical Indian, Pacific, and Atlantic oceans at the large (>500 to 1000 km) spatial and long (>1 to 2 months) temporal scales characteristic of major climatic events. Two new relations have been found between these fields, their role in large-scale climate dynamics in general, and the El Niño–Southern Oscillation in particular. First, there is a dramatic change in convection regimes that occurs at a critical SST of about 27.5°C (hereafter T_c) at many locations in the Indian and Pacific oceans. Specifically, we find that although SSTs in excess of T_c are required for deep convection to occur, the intensity of convection appears to be insensitive to further increases in surface temperature. Below T_c deep convection does not occur. This result confirms and extends the results reported by Gadgil *et al.* (*1*) for a portion of the tropical Indian Ocean. Data from the tropical Atlantic show similar structure though the critical temperature is slightly lower. Second, we find evidence that when SSTs are above T_c, surface wind divergence is closely associated with the presence or absence of deep convection. In some regions, convection appears to be suppressed by persistent divergent surface flow that reflects large-scale subsidence.

Scripps Institution of Oceanography, La Jolla, CA 92093.

These findings have important implications with respect to the physical understanding and parameterization of tropical convection and other atmospheric responses to SST changes. The rapid change in convective regimes that occurs in a relatively narrow range of temperatures may be of major importance in modulating the response of the coupled air-ocean system to changes in tropical SSTs via the release of latent heat to the atmosphere by large-scale tropical convection. Recent theoretical model results of Neelin and Held (*2*) and of Lau and Shen (*3*) support this idea. Also, the relation between surface wind divergence and convection and the existence of regions where convection is persistently suppressed at SSTs above T_c indicate that tropical convection is regulated at times by changes in vertical motion related to remote atmospheric events occurring in the tropics or extratropics.

The data used in the study cover the period January 1974 through December 1979. The SST data came originally from the Comprehensive Oceanographic Atmospheric Data Set (COADS) (*4*). The COADS data comprise more than 60 million ship observations that have been subjected to strict quality control. These data were then further processed to provide box averages for 4° by 4° regions (*5*). The surface wind data come from the Indo-Pacific data set assembled from ship observations (*6*). The ending of the current COADS data set in 1979 constrained the length of the study period. Results from work in progress with more recent data confirm the conclusions presented here.

Satellite measurements of outgoing longwave radiation (OLR) data were used as a surrogate for convection, as has been done by many workers (*7–10*). Its usefulness for this purpose results from the fact that upwelling thermal radiation emitted by the ocean surface is absorbed and reemitted by atmospheric water (vapor, droplets, or ice crystals). The amount of radiation reemitted is dependent on the temperature of the atmospheric water, which in turn is a function of altitude. The longwave radiation received at a satellite is thus an integrated measure of the distribution of water vapor with height. The sequence of multiple absorptions and reemissions results in a brightness temperature appropriate for a source located several thousand meters above sea level over the tropics. When large quantities of water are transported high into the atmosphere in deep tropical convective clouds, the altitude of the apparent emission source is raised, thereby lowering its brightness temperature. These regions appear as areas of lower (cooler) satellite-sensed OLR that can be distinguished from relatively warmer appearing areas free from convection.

Morressey (*11*) examined the relation between OLR and daily precipitation over the equatorial Pacific and found correlations ranging from about −0.5 to −0.6. These are significant at the 95% level for the samples tested. The relation between OLR and precipitation would probably be closer for the much longer averaging times (30 to 60 days rather than daily) used in our study. The major discrepancies between OLR and precipitation in (*11*) appeared to result from cases where cirrus clouds overlying shallow convective clouds produced cold OLR values that were indicative of deep convection, although heavy precipitation was not observed.

The OLR data used in this study come from scanning radiometers aboard polar-orbiting satellites operated by the National Oceanic and Atmospheric Administration (NOAA). The methods used to derive the

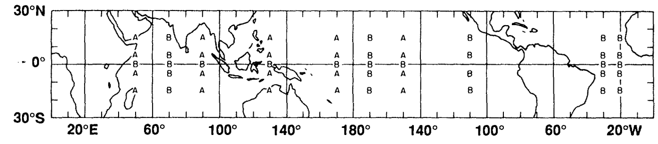

Fig. 1. Locations used in this study. Data in Figs. 2, 5, and 6 are from the locations marked A.

radiation values have been extensively described (*12*) and potential measurement problems have been discussed (*7, 8, 13*). Our data were gridded 5° by 5° averages for 5-day periods. These 5-day averages were filtered (*14*) to remove the 40- to 60-day oscillation known to be present in tropical OLR data (*8, 9*) because it seems unlikely that this signal is a direct response to local changes in SST. The filtered data were then processed to provide monthly data for comparison with the SST and wind data. No filtering was performed on the SST or wind data.

The local relations between convection and water temperature were examined by pairing colocated OLR and SST observations from 50 sites in the Indian, Pacific, and Atlantic oceans between 15°N and 15°S (Fig. 1). The data were displayed as simple scatter diagrams (Fig. 2), which are for the composite data from 20 locations in the tropical Indian and Pacific oceans (marked A in Fig. 1). The discontinuity at ~27.5°C is clearly apparent and is associated with an OLR value of ~240 W m^{-2}, a threshold level often used to mark deep convection in the tropics (*9, 10*). The pattern is similar to that for a different type of satellite cloud data from the tropical Indian Ocean (*1*). Bjerknes (*15*), Krueger and Gray (*16*), and Quiroz (*17*), among others, have drawn attention to the dependence of deep convection and precipitation on the presence of 28°C water in the equatorial Pacific.

The pattern shown in Fig. 2 does not result solely from the spatial distribution of the sample points; inspection of scatter plots prepared for the individual locations shows that the 27° to 28°C discontinuity is present at most locations where SSTs frequently crossed the critical temperature. The scatter diagrams for the various locations can be conveniently divided into four groups or types (Fig. 3): (i) Sites where SSTs remained above T_c—there was little relation between SST and OLR (*18*), although deep convection did occur (type W). (ii) Sites where SSTs remain below the T_c; deep convection (on monthly time scales) was not observed (type C). (iii) Sites where SSTs were often observed on either side of the transition temperature and that shared characteristics of types W and C above (type T). The data from these locations demonstrate that the pattern shown in Fig. 2 is not due solely to regional differences. (iv) Sites that showed clear evidence that deep convection was suppressed even when SSTs exceeded T_c (type S). Each type can be found in all three oceans, although the value of T_c appears to be somewhat lower (<27°C) in the Atlantic.

The geographic distribution of the four types of sites in the Indian and Pacific oceans is depicted in Fig. 4; we have added a regional interpretation of their spatial disposition. The regions show rough congruence with the annual mean isotherm of 27.5°C; that is, type W sites are inside the isotherm, type T sites are near the isotherm, and type C sites are at the poleward edges and in the eastern Pacific. The sites where convection appears to be persistently suppressed (type S) are located in the equatorial east-central Pacific, north of the Intertropical Convergence Zone and in the western Indian Ocean. Surface wind divergence data show that each of these three regions is marked by persistent divergence, indicating that large-scale subsidence suppresses convection in these areas.

The overall relation between SST and OLR for the locations used to prepare Fig. 2 is shown as a plot of mean OLR values for 0.5°C SST bins in Fig. 5. Composited in this way, the discontinuity appears as a smooth change from nonconvective to convective regimes between 26°C and 28°C. The confidence intervals suggest that the differences in the means over this range did not arise by chance. At temperatures between 24°C and 26°C the curve shows the expected decrease in OLR with decreasing surface temperatures. Furthermore, although equivalent brightness temperatures calculated from the measured OLR values are indicative of a virtual emission source in the midtroposphere, the change in OLR through the lower range agrees well with that calculated from the Stefan-Boltzmann

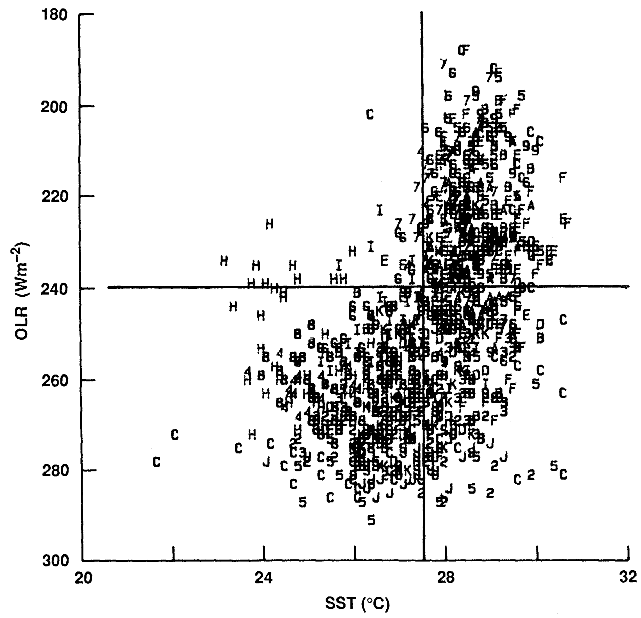

Fig. 2. Scatter plot of SST and OLR. OLR values decrease (convection increases) toward the top; SSTs are warmer to the right. Note the break at SSTs of ~27.5°C (vertical line) that is associated with OLR values of ~240 W m^{-2} (horizontal line), a threshold often associated with deep convection. Also note that there is little relation between SSTs and OLR when SSTs exceed 27.5°C. These are monthly data for 1974 to 1979. Separate symbols are used to represent different locations (this plot only). The site at 15°N, 50°E is not included.

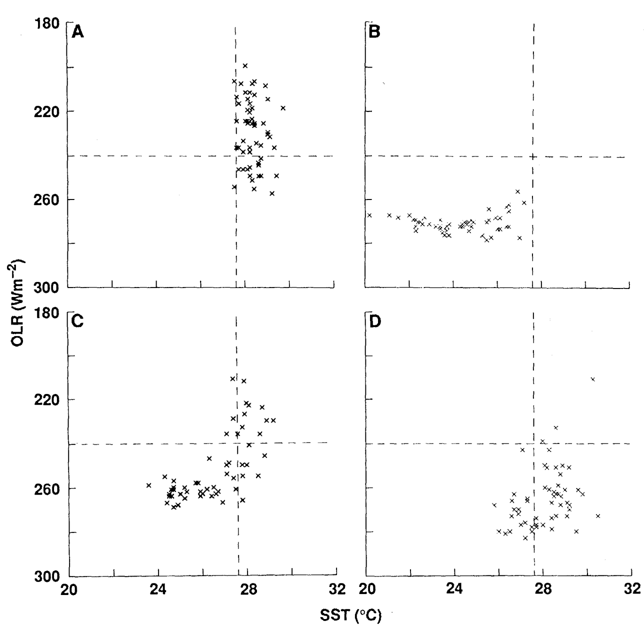

Fig. 3. As in Fig. 2 but for representatives of each type of SST-OLR relation. (**A**) Type W (5°N, 90°E); (**B**) type C (0°, 110°W); (**C**) type T (15°S, 50°E); and (**D**) type S (0°, 170°W).

equation. As noted previously, increases in SST once T_c is exceeded appear to have little effect on the level of convection, and in fact a downturn is suggested at high temperatures. The data are thus compatible with a null relation between SST and OLR above T_c (*18*).

Two additional features are of interest in Fig. 5. The population curve peaks at 28°C, the point at which SSTs no longer have much effect on convective activity. This suggests that 28°C represents an equilibrium tropical SST under convective conditions. Second, the population curve drops off rapidly from the 28°C peak with few instances of mean temperatures in excess of 30°C. These features support calculations by Newell (*19*) indicating that 30°C is an approximate upper limit to equilibrium tropical SSTs and are in agreement with histograms of tropical SSTs presented by Newell *et al.* (*20*) that portray such behavior. Newell's calculations (*19*) were made by assuming representative tropical ocean values for air temperature, relative humidity, and solar radiation with parameterized reradiation of longwave energy from atmospheric water vapor. The results shows that under clear skies and low wind speed conditions the equilibrium temperature was about 30°C. This value is determined in large part by a balance between latent heat losses, which increase rapidly with increasing SSTs, and incident solar radiation. Inspection of Newell's results shows that a reduction in solar radiation of about 30% due to clouds (a realistic value) would reduce the equilibrium temperature to the observed 28°C value. Thus our observations support the idea (*19–21*) that evaporative cooling and the cloud cover associated with convection place an upper limit on tropical SSTs, thereby acting as controllers for the large-scale circulation.

The role of surface wind divergence (*22*) in regulating the intensity of convection when SSTs exceed T_c is demonstrated by the bivariate histogram (Fig. 6), which shows that where the rapid decrease in mean OLR between SSTs of 26°C and 28°C occurs, surface wind divergence has little effect on convective activity, that is, the OLR contours are nearly parallel to the $\nabla \cdot \mathbf{U}$ axis. In contrast, when SSTs are above T_c and OLR values are less than 240 W m^{-2}, the sloping contours show an increasingly close relation between convection and surface divergence, as would be expected. This observation supports model results (*3*) that show moisture convergence rather than SST plays the dominant role in governing convection at SSTs above 28°C. It is apparent in Fig. 6, in published mean charts (*23*), and in scatter plots (*24*) that surface wind convergence shows only a loose relation with SSTs. This suggests that where SSTs are above T_c, remotely forced changes in vertical motion or stability or both play an important role in regulating convection (*25*).

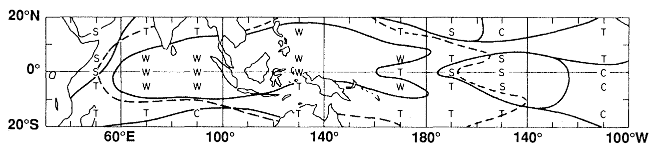

Fig. 4. Geographic distribution of locations in the Indian and Pacific oceans by appearance of SST-OLR scatter plots. The 27.5°C mean annual SST contour is dashed.

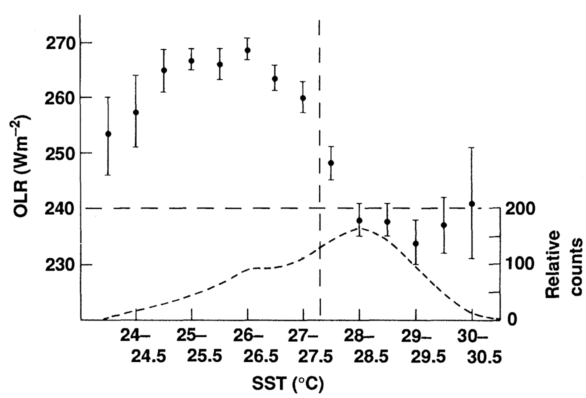

Fig. 5. Mean OLR values (vertical, convection increases downward) for 0.5°C SST bins shown on horizontal axis for data in Fig. 2. Error bars are for 95% confidence intervals for bin means estimated by the *t* test. Populations of SST bins is shown by dashed line; note the peak at 28°C and the rapid drop of between 28°C and 30°C.

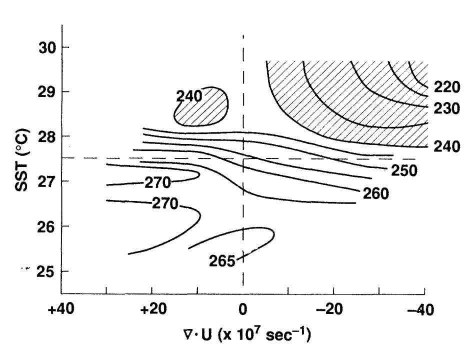

Fig. 6. Mean OLR values (contoured at 5 W m^{-2} intervals) for 0.5°C SST bins (vertical axis) and 10 × 10^{-7} sec^{-1} surface wind divergence bins (horizontal axis, negative values indicate convergent surface flow) for locations used to prepare Figs. 2 and 5. OLR values in less than 240 W m^{-2} are shaded. Note the increasingly close relation between divergence and convection when SSTs are above 28°C.

REFERENCES AND NOTES

1. S. Gadgil *et al.*, *Nature (London)* **312**, 141 (1984).
2. J. D. Neelin and I. M. Held, *Mon. Weather Rev.* **115**, 3 (1987).
3. K.-M. Lau and S. Shen, unpublished results.
4. R. J. Slutz *et al.*, *The Comprehensive Ocean-Atmosphere Data Set, Release 1* (Climate Research Program, Environmental Research Laboratory/National Oceanic and Atmospheric Administration, Boulder, CO, 1985); S. D. Woodruff, Ed., *Natl. Oceanic Atmos. Adm. (U.S.) Tech. Memo. ERL ESG-23* (1986).
5. P. Barbour, *Scripps Institution of Oceanography Reference No. 86-26* (Climate Research Group, Scripps Institution of Oceanography, University of California, San Diego, San Diego, 1986).
6. T. P. Barnett, *Mon. Weather Rev.* **111**, 756 (1983).
7. G. C. Griffith *et al.*, *ibid.* **106**, 1153 (1978).
8. K. M. Weickmann, *ibid.* **111**, 1838 (1983).
9. K.-M. Lau and P. H. Chan, *ibid.* **113**, 1889 (1985).
10. T. Murakami, *ibid.* **108**, 205 (1980).
11. M. L. Morressey, *ibid.* **114**, 931 (1986).
12. A. Gruber, *Natl. Oceanic Atmos. Adm. Tech. Rep. NESS 1976* (1977); ——— and J. Winston, *Bull. Am. Meteorol. Soc.* **59**, 1570 (1978).
13. D. L. Hartmann and D. A. Short, *J. Atmos. Sci.* **37**, 1233 (1980).
14. The filter was a cosine taper with a 30-day (six 5-day average observations) half width; the 0.1 power point was at 50 days.
15. J. Bjerknes, *Mon. Weather Rev.* **97**, 163 (1969).
16. A. F. Krueger and T. I. Gray, Jr., *ibid.*, p. 700.
17. R. S. Quiroz, *ibid.* **111**, 1685 (1983).
18. One might be tempted to fit a sharply sloping curve to the distribution in Fig. 2, which suggests a strong dependence of convection on SST above T_c. In fact, given the scatter in the data, we cannot rule out this possibility. However, associations between SSTs and OLR for SSTs above 28°C at applicable locations in Fig. 1 generally range between $r = 0.3$ and $r = +0.3$, and suggest that the dependence of the level of convection on SSTs in this temperature range is usually slight.
19. R. E. Newell, *Am. Sci.* **67**, 405 (1979).
20. R. E. Newell *et al.*, *Pure Appl. Geophys.* **116**, 351 (1978).
21. I. Hoffert *et al.*, *J. Atmos. Sci.* **40**, 1659 (1983).
22. The convergence data given here represent box averages for 6° latitude by 10° longitude regions centered on the point of interest.
23. R. E. Newell *et al.*, *The General Circulation of the Tropical Atmosphere and Interactions with Extratropical Latitudes* (MIT Press, Cambridge, MA, 1974), vol. 1; H. Riehl, *The Climate and Weather in the Tropics* (Academic Press, London, 1979), p. 20; J. Horel, *Mon. Weather Rev.* **110**, 1863 (1982).
24. Scatter plots show generally weak positive relations between SST and surface convergence with wide regional variability. An overall histogram for the composited data from the points used for Fig. 5 shows no significant increase in mean convergence with increasing SSTs above 27°C.
25. S. G. Philander *et al.*, *J. Atmos. Sci.* **41**, 604 (1984); J. K. Firestone and B. A. Albrecht, *Mon. Weather Rev.* **114**, 2219 (1986).
26. We thank K. Weickmann for kindly providing the OLR data used in this study and K. Weickmann, K.-M. Lau, J. Horel, B. Chertock, and R. Somerville for useful discussions and comments. This work was sponsored in part by the National Science Foundation under grant ATM85-13713.

26 May 1987; accepted 16 September 1987